Preparation and Molecular Stereochemistry of Six-Coordinate (Isothiocyanato)(pyridine)(porphinato)iron(III) Complexes. (Isothiocyanato)(*meso*-tetraphenylporphinato)(pyridine)-iron(III), a Low-Spin Complex with a Nonlinear Fe–N–C–S Group, and (Isothiocyanato)(octaethylporphinato)(pyridine)iron(III), a High-Spin Complex with Nonequivalent Axial Ligands

W. Robert Scheidt,*[1] Young Ja Lee,[1] David K. Geiger,[1] Karen Taylor,[1,2] and Keiichiro Hatano*[3]

Contribution from the Department of Chemistry, University of Notre Dame, Notre Dame, Indiana 46556, and the Department of Pharmaceutical Science, Nagoya City University, Nagoya, Japan 467. *Received October 26, 1981*

Abstract: The preparation and characterization of two six-coordinate (porphinato)iron(III) derivatives having the mixed-axial ligation of pyridine and isothiocyanate is described. One derivative, (isothiocyanato)(*meso*-tetraphenylporphinato)(pyridine)iron(III), Fe(TPP)(py)(NCS), is essentially a low-spin ($S = {}^1/_2$) complex while the second derivative, (isothiocyanato)(octaethylporphinato)(pyridine)iron(III), Fe(OEP)(py)(NCS), is a high-spin ($S = {}^5/_2$) complex. The crystal and molecular structure of the two complexes has been determined. The structure determination of Fe(OEP)(py)(NCS) is the first high-spin six-coordinate iron(III) porphyrinate having nonequivalent axial ligands to be characterized. The structure of Fe(TPP)(py)(NCS) is that expected for a low-spin (porphinato)iron(III) species with an average Fe–N_p distance of 1.988 (9) Å, Fe–N(py) = 2.082 (3) Å, and Fe–N(NCS) = 1.942 (4) Å. The Fe–N–C–S group is partly bent with an Fe–N–C angle of 155.6 (3)°. The bending is attributed to packing interactions in the solid state. The structure of Fe(OEP)(py)(NCS) shows an average increase in bond distance of 0.115 Å which is quite anisotropic in distribution: average Fe–N_p = 2.048 (4) Å, Fe–N(py) = 2.442 (2) Å, Fe–N(NCS) = 2.031 (2) Å. The iron(III) atom is displaced by 0.24 Å from the mean plane of the core toward the isothiocyanate ligand. The Fe–N–C–S group is linear. Crystal data for Fe(TPP)(py)(NCS): a = 13.238 (3) Å, b = 23.917 (5) Å, c = 14.269 (3) Å, and β = 104.74 (1)°, Z = 4, space group $P2_1/n$, 5878 unique observations used in the structure determination. Crystal data for Fe(OEP)(py)(NCS): a = 12.348 (3) Å, b = 15.625 (4) Å, c = 10.535 (2) Å, and α = 92.30 (2)°, β = 105.10 (2)°, γ = 101.10 (2)°, Z = 2, space group $P\bar{1}$, 7549 unique reflections.

Thiocyante, NCS^-, is a linear ambidentate ligand[4] which can bind to metals either via its nitrogen or its sulfur atom. When N bound, the M–NCS group is generally linear, and when S bound, the M–S–C angle is bent (~110°). The mode of coordination depends on the metal ion, the other ligands of the metal,[4] and stereochemical factors.[5]

Recently Korszun and Moffat[6] have determined the structure of thiocyanato-ligated hemoglobin. Some of their results are unexpected in terms of the normal coordination behavior of thiocyanate. In (NCS)MetHb,[7] the thiocyanate ligand is bound to the iron of heme through the nitrogen atom but with a distinctly nonlinear geometry (Fe–N–C angle = 120 ± 10°). Indeed, the coordination geometry is quite similar to that displayed by the azide analogue (N_3)MetHb.[8] This nonlinear geometry is apparently required for the thiocyanate ligand to fit into the ligand binding pocket of hemoglobin. Thus, for example, there are observed perturbations for hemoprotein derivatives such as (CN)MetHb[9] which would ordinarily have linearly bound ligands. The steric problems of thiocyanate binding in the heme pocket would be alleviated for an S-bound ligand.

Bloom and Hoard[10] have determined the structure of the five-coordinate thiocyanato-ligated (porphinato)iron(III) complex, Fe(TPP)(NCS). This complex has a N-bonded linear Fe–NCS group. We have synthesized and determined the molecular stereochemistry of a six-coordinate species, (isothiocyanato)-(*meso*-tetraphenylporphinato)(pyridine)iron(III), Fe(TPP)-(py)(NCS), to determine the effects of the presence of the sixth ligand on the mode of thiocyanate binding and its geometry. This complex has an N-bonded isothiocyanate with a somewhat bent Fe–NCS group; the Fe–N–C angle is 155.6 (3)°. The bending of the group appears to result from packing considerations; significantly shorter intermolecular contacts between the NCS atoms and other atoms would result if the Fe–NCS group were linear.[11] We have also examined a number of other reported complexes in which nonlinear M–NCS groups occur. In all cases, model

(1) University of Notre Dame.
(2) NSF URP participant, Summer 1981.
(3) Nagoya City University.
(4) Norbury, A. H. *Adv. Inorg. Chem. Radiochem.* **1975**, *17*, 231–386. Burmeister, J. L. In "The Chemistry and Biochemistry of Thiocyanic Acid and its Derivatives"; Newman, A. A., Ed.; Academic Press: London, 1975; Chapter 2.
(5) Palenik, G. J.; Mathew, M.; Steffen, W. L.; Beran, G. *J. Am. Chem. Soc.* **1975**, *97*, 1059–1066.
(6) Korszun, Z. R.; Moffat, K. *J. Mol. Biol.* **1981**, *145*, 815–824.
(7) Abbreviations used in this paper: MetHb, methemoglobin; TPP, dianion of *meso*-tetraphenylporphyrin; OEP, dianion of octaethylporphyrin; Porph, dianion of a generalized porphyrin; py, pyridine; 3-Clpy, 3-chloropyridine; 4-Mepy, 4-methylpyridine; terpyr, terpyridine; N_p, porphinato nitrogen atom.
(8) Deatherage, J. F.; Loe, R. S.; Moffat, K. *J. Mol. Biol.* 1979, *134*, 419–429.
(9) Deatherage, J. F.; Loe, R. S.; Andersen, C. M.; Moffat, K. *J. Mol. Biol.* **1976**, *104*, 723–728.
(10) Bloom, A.; Hoard, J. L. "Abstracts of Papers", 173rd National Meeting of the American Chemical Society, New Orleans, LA, March 21–25, 1977; American Chemical Society: Washington, D.C., 1977; INORG 27.
(11) In all calculations of such nonbonded contacts, the assumption that no other structural reorganization would occur was made. This is clearly an oversimplification but should nonetheless give some measure of nonbonded interaction effects.

0002-7863/82/1504-3367$01.25/0

calculations suggest that nonbonded repulsions could play a part in the deviation from linearity.

Thiocyanato complexes of methemoglobin are known[12,13] to possess magnetic moments higher than those expected for a pure low-spin state. Magnetic measurements for Fe(TPP)(py)(NCS) yield moments, at room temperature, higher than those expected for a pure low-spin complex. This observation suggests that the axial ligand combination, isothiocyanate and pyridine, brings the iron(III) porphyrinate derivatives close to the spin crossover point between the low-spin and high-spin ground states.

We have explored this observation by synthesizing and characterizing a related complex, (isothiocyanato)(octaethylporphinato)(pyridine)iron(III), Fe(OEP)(py)(NCS). This complex is *high-spin* at all temperatures down to 77 K. We have determined the molecular stereochemistry of this species by X-ray diffraction. The complex is indeed six-coordinate and represents the first structural characterization of a high-spin ferric porphyrinate having nonidentical axial ligands. We have thus prepared two (porphinato)iron(III) complexes with identical axial ligands, one having essentially a low-spin state and a second having a high-spin ground state. The structures of the two species are compared particularly in regard to the possible structural changes in the coordination groups of hemoproteins undergoing thermal spin equilibria.[14]

Experimental Section

Synthesis and Characterization of Fe(TPP)(py)(NCS). Fe(TPP)(NCS) was prepared by shaking a chloroform solution of $[Fe(TPP)]_2O$ (0.5 g/150 mL) with an acidified aqueous solution of KNCS.[15] Crystalline Fe(TPP)(NCS) was obtained upon addition of *n*-pentane. Fe(TPP)(py)(NCS) was prepared by dissolving 100 mg of Fe(TPP)(NCS) in 2 mL of $CHCl_3$ and 5 mL of dry pyridine. After undissolved material was filtered off through a cotton frit, single crystals of Fe(TPP)(py)(NCS)·$^1/_2$py were obtained by allowing *n*-pentane to diffuse slowly into the solution. The solvent ratios are important: smaller amounts of pyridine lead to materials of different, and unknown, composition. Anal. Calcd for $C_{52.5}H_{35.5}N_{6.5}FeS$: C, 74.60; H, 4.23; N, 10.77. Found: C, 74.26; H, 4.16; N. 10.24.

Infrared spectra were obtained as KBr pellets on a JASCO IRA-2 spectrometer. In Fe(TPP)(py)(NCS), the NCS stretching region has a peak at 2010 cm^{-1} and a shoulder at 2050 cm^{-1}. Fe(TPP)(NCS) has a peak at 2000 cm^{-1} and "free NCS" (in $[Fe(TPP)(1\text{-MeIm})_2]NCS$) has a single sharp peak at 2050 cm^{-1}. NMR spectra were measured on JEOL FX-100 in the FT mode with probe temperatures determined with a copper constantan thermocouple. Solution susceptibilities were determined on a Varian EM-390; the probe temperature was measured by using the methanol thermometer.

Magnetic moments were measured in solution[16] and in the crystalline state. In solution (10% py in $CHCl_3$), the susceptibility shows a marked temperature dependence: 311 K, 4.8 μ_B; 308 K, 4.7 μ_B; 303 K, 4.4 μ_B; 282 K, 3.3 μ_B; 270 K, 2.7 μ_B; 261 K, 2.1 μ_B. In the solid state, the susceptibilities display a smaller temperature dependence: 295 K, 3.67 μ_B; 177 K, 3.54 μ_B; 126 K, 3.24 μ_B; 103 K, 3.20 μ_B; 77 K, 3.04 μ_B.

Synthesis of Fe(OEP)(py)(NCS). Fe(OEP)(NCS) was prepared in a similar fashion as Fe(TPP)(NCS). Fe(OEP)(py)(NCS) was prepared by dissolving 300 mg of Fe(OEP)(NCS) in 20 mL of $CHCl_3$, 2 mL of pyridine was added, and *n*-pentane was allowed to slowly diffuse into the solution. A mixture of powdery material and fine crystalline material was formed in the flask. Only the crystalline material was collected and recrystallized from 2:1 $CHCl_3$–pyridine. Several crystallizations afforded crystals suitable for X-ray analysis: yield 100 mg; IR ν(NCS) 2038 cm^{-1}. Anal. Calcd for $C_{42}H_{53}N_6SFe$: C, 69.12; H, 7.32; N, 11.52. Found: C, 69.70; H, 6.68; N, 11.53. In the solid state, $\mu_{eff}^{26°C}$ = 5.9 μ_B and was independent of temperature to 77 K.

Structure Determination of Fe(TPP)(py)(NCS). Preliminary X-ray study of crystals of Fe(TPP)(py)(NCS) on a Syntex P$\bar{1}$ automated diffractometer established a four-molecule monoclinic unit cell. Crystal data are summarized in Table I. Intensity data were collected by using graphite-monochromated Mo Kα radiation ($\bar{\lambda}$ = 0.710 73 Å). A summary of the intensity collection parameters are given in Table I. The intensities of four standard reflections were measured every 50 reflections to monitor the alignment and possible deterioration of the crystal during data collection. No significant variation in the standard intensities was observed. Intensity data were reduced as previously described.[17] No absorption correction was made (μ = 0.43 mm^{-1}).

Table I. Summary of Crystal Data and Intensity Collection Parameters

	Fe(TPP)(py)(NCS)·$^1/_2$py	Fe(OEP)(py)(NCS)
formula	$FeSN_{6.5}C_{52.5}H_{35.5}$	$FeSN_6C_{42}H_{49}$
fw, amu	845.3	725.8
space group	$P2_1/n$	$P\bar{1}$
temp, °C	19 ± 1	19 ± 1
a, Å	13.238 (3)	12.348 (3)
b, Å	23.917 (5)	15.625 (4)
c, Å	14.269 (3)	10.535 (2)
α, deg	90.0	92.30 (2)
β, deg	104.74 (1)	105.10 (2)
γ, deg	90.0	101.10 (2)
Z	4	2
d(calcd), g/cm^3	1.285	1.257
d(obsd), g/cm^3	1.294	1.255
radiation	graphite monochromated Mo Kα (λ = 0.710 73 Å)	
scan technique	θ–2θ	θ–2θ
cryst dimens, mm	0.3 × 0.4 × 0.7	0.2 × 0.3 × 0.7
scan range	0.75° below Kα_1 0.75° above Kα_2	0.4° below Kα_1 0.4° above Kα_2
scan rate, deg/min	2–12	2–12
bkgd	0.5 time scan time at the extremes of scan	
2θ limits, deg	3.5–50.67	3.5–54.7
criterion for observn	$F_o > 3\sigma(F_o)$	
unique obsd data	5878	7549
μ, mm^{-1}	0.43	0.48
R_1	0.066	0.052
R_2	0.078	0.069
goodness of fit	2.29	2.02
data/parameter	11.2	16.4

The structure was solved by the usual heavy-atom method.[18] A series of difference Fourier syntheses revealed the positions of all heavy atoms except those of the pyridine solvate. After several cycles of block-diagonal least-squares refinement, a difference Fourier synthesis showed electron density about the special positions 0, 0, 0 and $^1/_2$, $^1/_2$, $^1/_2$. This electron density was assumed to be a disordered pyridine solvate. The pyridine solvate molecule was refined by rigid-group methods; a six-membered ring with D_{6h} symmetry, C–C distances of 1.395 Å, and occupancy factors of 0.5 for each atom was used. Subsequent difference Fourier maps showed electron density in positions appropriate for the hydrogen atoms of the molecule. All hydrogen atoms, except those of the solvate, were assigned to their idealized positions, with *d*(C–H) = 0.95 Å. The thermal parameters were fixed one unit higher than the bonded carbon atom. With the 33 hydrogen atoms included as fixed contributors, the structure was then refined to convergence by using anisotropic temperature factors for the heavy atoms. The idealized hydrogen atom positions were adjusted as required during the refinement. The final value of R_1 was 0.066 and R_2 was 0.078.[19] A final difference Fourier had five peaks (0.5–0.7 e/Å^3) near the iron atom; the map was otherwise judged to be featureless. A final listing of observed and calculated structure factors is available as supplementary material. Final atomic coordinates are listed in Table II. The associated anisotropic thermal parameters are listed in Table III (supplementary material).

Structure Determination of Fe(OEP)(py)(NCS). X-ray study of crystals of Fe(OEP)(py)(NCS) established a two-molecule triclinic unit

(12) Perutz, M. F.; Sanders, J. K. M.; Chenery, D. H.; Noble, R. W.; Pennelly, R. R.; Fung, L. W.-M.; Ho, C.; Giannini, I.; Porschke, D.; Winkler, H. *Biochemistry* **1978**, *17*, 3640–3652.

(13) Messana, C.; Cerdonio, M.; Shenkin, R.; Noble, R. W.; Fermi, G.; Perutz, R. N.; Perutz, M. F. *Biochemistry* **1978**, *17*, 3652–3662.

(14) Iizuka, T.; Yonetani, T. *Adv. Biophys.* **1970**, *1*, 157–186. See also references cited in: Huang, Y.-P.; Kassner, R. J. *J. Am. Chem. Soc.* **1981**, *103*, 4297–4932 and references cited in 26.

(15) Maricondi, C.; Swift, W.; Straub, D. K. *J. Am. Chem. Soc.* **1969**, *91*, 5205–5210.

(16) Evans, D. F. *J. Chem. Soc.* **1959**, 2003–2005.

(17) Scheidt, W. R. *J. Am. Chem. Soc.* **1974**, *96*, 84–89.

(18) Programs used in this study included local modifications of Jacobson's ALFF and ALLS, Busing and Levy's ORFFE and ORFLS, and Johnson's ORTEP2. Atomic form factors were from: Cromer, D. T.; Mann, J. B. *Acta Crystallogr., Sect. A.* **1968**, *24*, 321–323, with real and imaginary corrections for anomalous dispersion in the form factor of the iron and sulfur atoms from: Cromer, D. T.; Liberman, D. J. *J. Chem. Phys.* **1970**, *53*, 1891–1898. Scattering factors for hydrogen were from: Stewart, R. F.; Davidson, E. R.; Simpson, W. T. *Ibid.* **1965**, *42*, 3175–3187.

(19) $R_1 = \sum||F_o| - |F_c||/\sum|F_o|$ and $R_2 = [\sum w(|F_o| - |F_c|)^2/\sum w(F_o)^2]^{1/2}$.

Table II. Fractional Atomic Coordinates in the Unit Cell[a]

atom	10^4x	10^4y	10^4z
Fe[b]	1518 (0)	3026 (0)	−1191 (0)
S	786 (2)	4125 (1)	−3928 (1)
N_1	642 (2)	2372 (1)	−1775 (2)
N_2	462 (2)	3230 (1)	−478 (2)
N_3	2430 (2)	3651 (1)	−561 (2)
N_4	2598 (2)	2807 (1)	−1856 (2)
N_5	2265 (2)	2500 (1)	−64 (2)
N_6	896 (2)	3508 (1)	−2281 (2)
C_{a1}	962 (3)	1922 (2)	−2222 (3)
C_{a2}	−351 (3)	2244 (2)	−1694 (3)
C_{a3}	−550 (3)	3026 (2)	−649 (3)
C_{a4}	552 (3)	3651 (2)	197 (3)
C_{a5}	2305 (3)	3975 (1)	204 (3)
C_{a6}	3331 (3)	3837 (1)	−774 (3)
C_{a7}	3400 (3)	3136 (2)	−2001 (3)
C_{a8}	2614 (3)	2324 (2)	−2369 (3)
C_{b1}	148 (3)	1508 (2)	−2440 (3)
C_{b2}	−652 (3)	1709 (2)	−2125 (3)
C_{b3}	−1093 (3)	3341 (2)	−78 (3)
C_{b4}	−427 (3)	3714 (2)	451 (3)
C_{b5}	3179 (3)	4347 (2)	498 (3)
C_{b6}	3799 (3)	4266 (2)	−107 (3)
C_{b7}	3893 (3)	2858 (2)	−2668 (3)
C_{b8}	3441 (3)	2357 (2)	−2864 (3)
C_{m1}	−935 (3)	2564 (2)	−1200 (3)
C_{m2}	1424 (3)	3988 (2)	560 (3)
C_{m3}	3751 (3)	3626 (2)	−1513 (3)
C_{m4}	1912 (3)	1881 (2)	−2480 (3)
C_1	−2011 (3)	2362 (2)	−1211 (3)
C_2	−2798 (3)	2347 (2)	−2080 (4)
C_3	−3776 (4)	2157 (2)	−2094 (5)
C_4	−3988 (4)	2001 (2)	−1273 (6)
C_5	−3258 (5)	2000 (3)	−426 (5)
C_6	−2248 (4)	2196 (2)	−408 (4)
C_7	1363 (3)	4404 (2)	1325 (3)
C_8	1093 (3)	4952 (2)	1088 (3)
C_9	945 (3)	5322 (2)	1780 (4)
C_{10}	1085 (4)	5158 (2)	2715 (4)
C_{11}	1379 (4)	4625 (2)	2959 (3)
C_{12}	1527 (4)	4245 (2)	2275 (3)
C_{13}	4634 (3)	3937 (2)	−1749 (3)
C_{14}	5618 (3)	3711 (2)	−1608 (3)
C_{15}	6406 (3)	3991 (2)	−1878 (4)
C_{16}	6217 (4)	4501 (2)	−2292 (4)
C_{17}	5263 (4)	4742 (2)	−2434 (4)
C_{18}	4462 (3)	4458 (2)	−2149 (4)
C_{19}	2197 (3)	1344 (2)	−2877 (3)
C_{20}	2956 (4)	1014 (2)	−2293 (4)
C_{21}	3255 (4)	510 (2)	−2639 (4)
C_{22}	2797 (4)	345 (2)	−3556 (4)
C_{23}	2050 (4)	666 (2)	−4146 (4)
C_{24}	1758 (3)	1165 (2)	−3806 (3)
C_{25}	1745 (3)	2100 (2)	280 (3)
C_{26}	2233 (4)	1711 (2)	943 (4)
C_{27}	3301 (4)	1741 (2)	1296 (4)
C_{28}	3828 (3)	2145 (2)	974 (4)
C_{29}	3298 (3)	2519 (2)	298 (3)
C_{30}	878 (3)	3765 (2)	−2961 (3)
C_{31}[c]	−178	−17	51
C_{32}[c]	149	−575	75
C_{33}[c]	1121	−703	−83
C_{34}[c]	1765	−274	−264
C_{35}[c]	1438	283	−288
C_{36}[c]	466	412	−131

[a] The numbers in parentheses are the estimated standard deviations in the least significant figure. [b] For Fe 10^5x = 15 186 (4), 10^5y = 30 257 (2), and 10^5z = −11 914 (4). [c] These are disordered solvent parameters derived from group refinement. The solvent molecule was given a fixed group thermal parameter of B = 22.6 Å^2 and occupancy factor of 0.5.

cell. A Delaunay reduction did not show any hidden symmetry. Crystal data and intensity collection parameters are summarized in Table I.

The space group $P\bar{1}$ was assumed. All subsequent developments during the solution and refinement of structure were consistent with this initial assumption. The structure was solved by using the direct methods program MULTAN78.[20] After several cycles of block-diagonal least-squares refinement, unrealistic positions of one peripheral ethyl group persisted. A difference Fourier synthesis suggested disorder in the group (C_{81} and C_{82}). Two positions for the β-carbon atoms of the group appeared consistent with the Fourier. These two atoms (C_{82a} and C_{82b}) were included in subsequent cycles of least-squares refinement with occupancy factors of 0.55 and 0.45. Subsequent difference Fourier maps showed electron density maxima in positions appropriate for the hydrogen atoms of the molecule. These hydrogen atoms were treated as before, with idealized C–H geometries (d(C–H) = 0.95 Å). The structure was then refined to convergence by using anisotropic temperature factors for all heavy atoms. The final value of R_1 was 0.052 and of R_2 was 0.069. A final difference Fourier synthesis has three peaks (0.60–0.49 e/Å^3) near the disordered ethyl group; the map was otherwise judged to be featureless. A final listing of observed and calculated structure amplitudes is available as supplementary material. The final atomic coordinates are given in Table IV. The final values of the associated thermal parameters are listed in Table V (supplementary material).

Table IV. Fractional Atomic Coordinates in the Unit Cell[a]

atom	10^4x	10^4y	10^4z
Fe[b]	3907 (0)	7424 (0)	1413 (0)
S[c]	6231 (0)	7614 (0)	−1626 (0)
N_1	2871 (2)	8171 (1)	359 (2)
N_2	4825 (2)	8513 (1)	2658 (2)
N_3	4770 (2)	6662 (1)	2671 (2)
N_4	2795 (2)	6310 (1)	412 (2)
N_5	4940 (2)	7497 (1)	186 (2)
N_6	2598 (2)	7358 (1)	2807 (2)
C_6	5474 (2)	7548 (1)	−567 (2)
C_{m1}	1441 (2)	6999 (2)	−1113 (2)
C_{m2}	3875 (2)	9613 (1)	1508 (2)
C_{m3}	6087 (2)	7818 (2)	4294 (2)
C_{m4}	3762 (2)	5214 (1)	1536 (2)
C_{a1}	1899 (2)	7879 (1)	−660 (2)
C_{a2}	3009 (2)	9065 (1)	534 (2)
C_{a3}	4716 (2)	9361 (1)	2501 (2)
C_{a4}	5708 (2)	8545 (1)	3781 (2)
C_{a5}	5675 (2)	6943 (1)	3774 (2)
C_{a6}	4634 (2)	5762 (1)	2499 (2)
C_{a7}	2894 (2)	5455 (1)	584 (2)
C_{a8}	1836 (2)	6269 (2)	−623 (2)
C_{b1}	1408 (2)	8604 (1)	−1150 (2)
C_{b2}	2087 (2)	9339 (1)	−407 (2)
C_{b3}	5563 (2)	9951 (1)	3551 (2)
C_{b4}	6168 (2)	9443 (1)	4347 (2)
C_{b5}	6125 (2)	6209 (2)	4314 (2)
C_{b6}	5498 (2)	5477 (1)	3506 (2)
C_{b7}	1964 (2)	4867 (2)	−351 (3)
C_{b8}	1310 (3)	5365 (2)	−1103 (3)
C_{11}	332 (2)	8538 (2)	−2254 (3)
C_{21}	1950 (2)	10275 (2)	−543 (3)
C_{31}	5723 (2)	10934 (1)	3657 (2)
C_{41}	7132 (2)	9728 (2)	5582 (2)
C_{51}	7109 (2)	6266 (2)	5531 (2)
C_{61}	5668 (2)	4555 (2)	3565 (2)
C_{71}	1782 (3)	3878 (2)	−450 (3)
C_{81}	238 (4)	5071 (2)	−2254 (5)
C_{12}	−741 (3)	8318 (3)	−1821 (4)
C_{22}	2554 (4)	10718 (2)	−1482 (4)
C_{32}	6408 (3)	11354 (2)	2767 (3)
C_{42}	8312 (2)	9870 (2)	5358 (3)
C_{52}	8258 (3)	6536 (2)	5274 (3)
C_{62}	6306 (3)	4319 (2)	2605 (3)
C_{72}	2364 (5)	3512 (2)	−1322 (4)
C_{82a}	189 (5)	5106 (4)	−3394 (6)
C_{82b}	−701 (5)	5000 (4)	−2074 (6)
C_1	1674 (3)	7712 (2)	2512 (3)
C_2	916 (3)	7666 (2)	3269 (4)
C_3	1125 (3)	7251 (2)	4414 (4)
C_4	2056 (3)	6891 (2)	4715 (3)
C_5	2776 (3)	6963 (2)	3914 (3)

[a] The numbers in parentheses are the estimated standard deviations in the least significant figure. [b] For Fe 10^5x = 39 073 (3), 10^5y = 74 242 (2), and 10^5z = 14 133 (3). [c] For S 10^5x = 62 310 (7), 10^5y = 76 140 (5), and 10^5z = −16 261 (8).

(20) A local modification of Main, Hull, Lessinger, Germain, Declerq, and Woolfson's MULTAN78 was used.

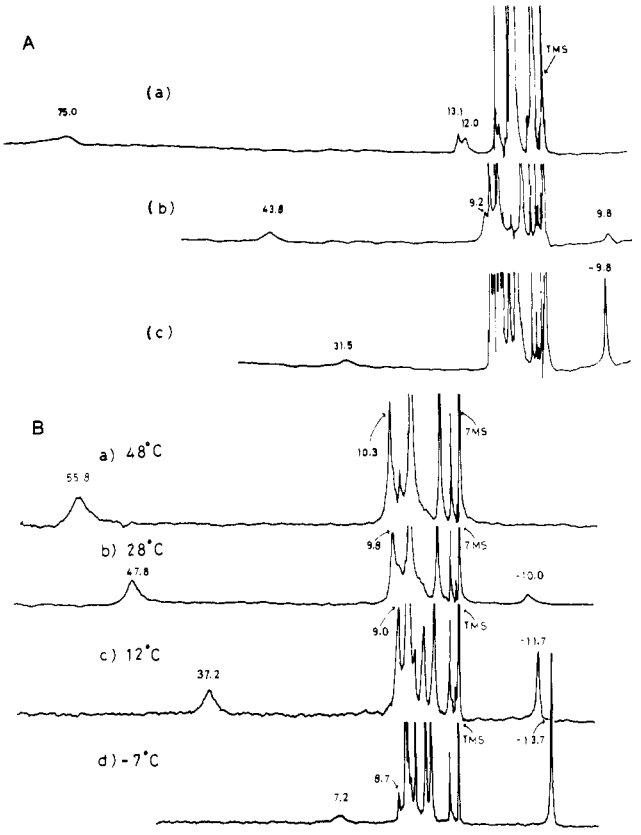

Figure 1. (A) The effect of pyridine concentration on the ^1H NMR spectra of Fe(TPP)(py)(NCS): $CHCl_3$ solutions with (a) 0% pyridine, (b) 10% pyridine, and (c) 30% pyridine at 20 °C. (B) The temperature dependenceof the ^1H NMR spectra in 10% pyridine–$CHCl_3$ solution. Temperatures of the individual spectra are indicated in the figure.

Results and Discussion

Synthetic Aspects. The preparation of (porhinato)iron(III) complexes having two nonequivalent axial ligands such as Fe(Porph)(X)(B), where X = anion and B = nitrogen ligand, is a synthetic challenge. The addition of a neutral ligand to a (porphinato)iron(III) complex can occur in two steps.

$$\text{Fe(Porph)(X)} + \text{B} \underset{}{\overset{K_1}{\rightleftharpoons}} \text{Fe(Porph)(X)(B)}$$

$$\text{Fe(Porph)(X)(B)} + \text{B} \overset{K_2}{\rightleftharpoons} \text{Fe(Porph)(B)}_2{}^+\text{X}^-$$

In general for most anions, $K_2 >> K_1$, and only the second product, with two equivalent axial ligands, is observed.[21,22] However, isolable complexes have been previously obtained for the cases where X = azide[23] and X = cyanide[24] and B = pyridine. Successful preparations can be obtained only in those cases where the first equilibrium constant is small. This requirement severely limits the choice of the nitrogen ligand and, to a lesser extent, the choice of anion. The small equilibrium constant for Fe(TPP)(NCS) + py ⇄ Fe(TPP)(py)(NCS), along with complications resulting from the varying spin state of the product prevents accurate spectrophotometric characterization of this complex in solution.

Infrared spectra of the various thiocyanate derivatives appears to provide some information concerning coordination of the thiocyanate ligand and the spin state of the complex. Coordinated NCS in five-coordinate and low-spin six-coordinate species yields thiocyanate frequencies that are significantly lower than those of "free" NCS with ν(NCS) of 2000 and 2010 cm^{-1}, respectively. In high-spin Fe(OEP)(py)(NCS), the NCS frequency (2038 cm^{-1}) is significantly closer to that of "free" NCS. The differences in the thiocyanate stretching frequencies for the low- and high-spin derivatives is similar to that observed for azide derivatives of myoglobin and hemoglobin. In these spin equilibrium hemoprotein derivatives, two different azide stretching frequencies are observed,[25] the peak at ~22 cm^{-1} higher frequency is associated with the high-spin form.

^1H NMR spectra of Fe(TPP)(NCS) as a function of pyridine concentration (at 20 °C) and as a function of temperature, as displayed in Figure 1, suggest complicated equilibria in solution. The downfield shifts (55.8–17.2 ppm) are associated with chemical exchange of high-spin Fe(TPP)(NCS) and Fe(TPP)(py)(NCS) (spin state uncertain, possibly a mixture of low and high spin). The upfield shifts (−9.8 to −13.7 ppm) are due to the presence of low-spin $[Fe(TPP)(py)_2]^+$. The successful isolation of the mixed-ligand six-coordinate species from solutions of high pyridine concentration may thus be the result of solubility considerations. These NMR results thus also explain the solution magnetic susceptibilities; the sharp decrease in moment with decreasing temperature is the result of an increasing concentration of (pre-

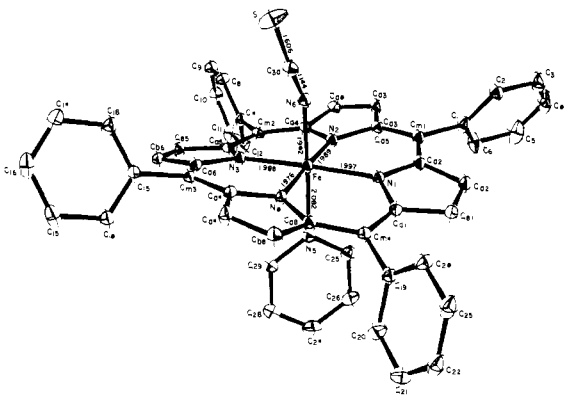

Figure 2. A perspective view of the Fe(TPP)(py)(NCS) molecule as it exists in the crystal. Also shown in the figure are the labels assigned to each atom and the bond distances in the coordination group. Atoms are contoured at the 50% probability level.

Table VI. Bond Lengths (Å) in the FeTPP(py)(NCS) Molecule[a]

$Fe-N_1$	1.997 (3)	$C_{a4}-C_{m2}$	1.395 (5)	C_7-C_8	1.378 (5)
$Fe-N_2$	1.989 (3)	$C_{a5}-C_{b5}$	1.435 (5)	C_7-C_{12}	1.371 (6)
$Fe-N_3$	1.988 (3)	$C_{a5}-C_{m2}$	1.386 (5)	C_8-C_9	1.375 (6)
$Fe-N_4$	1.976 (3)	$C_{a6}-C_{b6}$	1.428 (5)	C_9-C_{10}	1.357 (6)
$Fe-N_5$	2.082 (3)	$C_{a6}-C_{m3}$	1.404 (5)	$C_{10}-C_{11}$	1.353 (6)
$Fe-N_6$	1.942 (4)	$C_{a7}-C_{b7}$	1.446 (5)	$C_{11}-C_{12}$	1.383 (6)
N_1-C_{a1}	1.372 (4)	$C_{a7}-C_{m3}$	1.382 (5)	$C_{13}-C_{14}$	1.376 (5)
N_1-C_{a2}	1.384 (4)	$C_{a8}-C_{b8}$	1.449 (5)	$C_{13}-C_{18}$	1.365 (6)
N_2-C_{a3}	1.387 (4)	$C_{a8}-C_{m4}$	1.392 (5)	$C_{14}-C_{15}$	1.376 (6)
N_2-C_{a4}	1.378 (4)	$C_{b1}-C_{b2}$	1.340 (5)	$C_{15}-C_{16}$	1.350 (6)
N_3-C_{a5}	1.382 (4)	$C_{b3}-C_{b4}$	1.344 (5)	$C_{16}-C_{17}$	1.355 (7)
N_3-C_{a6}	1.378 (4)	$C_{b5}-C_{b6}$	1.347 (5)	$C_{17}-C_{18}$	1.404 (6)
N_4-C_{a7}	1.378 (4)	$C_{b7}-C_{b8}$	1.337 (5)	$C_{19}-C_{20}$	1.379 (6)
N_4-C_{a8}	1.370 (4)	$C_{m1}-C_1$	1.500 (5)	$C_{19}-C_{24}$	1.374 (6)
N_5-C_{25}	1.344 (5)	$C_{m2}-C_7$	1.495 (5)	$C_{20}-C_{21}$	1.399 (6)
N_5-C_{29}	1.333 (4)	$C_{m3}-C_{13}$	1.495 (5)	$C_{21}-C_{22}$	1.353 (7)
N_6-C_{30}	1.144 (5)	$C_{m4}-C_{19}$	1.491 (5)	$C_{22}-C_{23}$	1.361 (7)
$C_{a1}-C_{b1}$	1.439 (5)	C_1-C_2	1.402 (6)	$C_{23}-C_{24}$	1.380 (6)
$C_{a2}-C_{m4}$	1.400 (5)	C_1-C_6	1.325 (6)	$C_{25}-C_{26}$	1.366 (6)
$C_{a2}-C_{b2}$	1.432 (5)	C_2-C_3	1.368 (6)	$C_{26}-C_{27}$	1.378 (7)
$C_{a2}-C_{m1}$	1.399 (5)	C_3-C_4	1.326 (9)	$C_{27}-C_{28}$	1.340 (7)
$C_{a3}-C_{b3}$	1.432 (5)	C_4-C_5	1.341 (9)	$C_{28}-C_{29}$	1.370 (6)
$C_{a3}-C_{m1}$	1.375 (5)	C_5-C_6	1.410 (7)	$C_{30}-S$	1.606 (5)
$C_{a4}-C_{b4}$	1.439 (5)				

[a] The numbers in parentheses are the estimated standard deviations in the least significant figure.

(21) Walker, F. A.; Lo, M.; Ree, M. T. *J. Am. Chem. Soc.* **1976**, *98*, 552–5560.
(22) Satterlee, J. D.; LaMar, G. N.; Frye, J. S. *J. Am. Chem. Soc.* **1976**, *98*, 7275–7282.
(23) Adams, K. M.; Rasmussen, P. G.; Scheidt, W. R.; Hatano, K. *Inorg. Chem.* **1979**, *18*, 1892–1899.
(24) Scheidt, W. R.; Luangdilok, W.; Haller, K. J.; Lee, Y. J.; Hatano, K., to be submitted for publication.
(25) McCoy, S.; Caughey, W. S. *Biochemistry* **1970**, *9*, 2387–2393. Alben, J. O.; Fager, L. Y. *Ibid.* **1972**, *11*, 842–847.

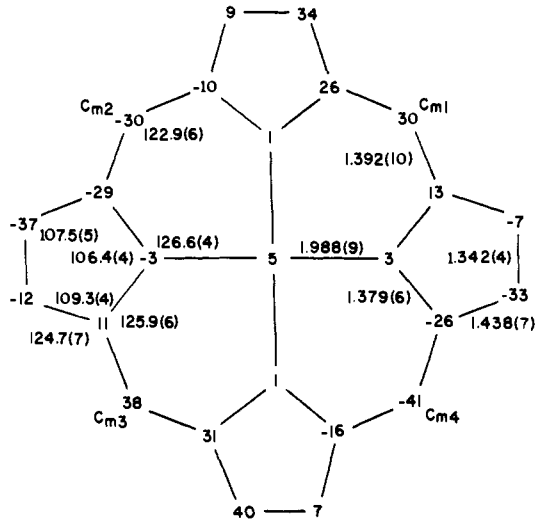

Figure 3. A formal diagram of the porphinato core of Fe(TPP)(py)(NCS) displaying the perpendicular displacements, in units of 0.01 Å, of each atom from the mean plane of the 24-atom core. The atom labels have been replaced by the value of the displacement; the orientation of the core is the same as in Figure 2.

sumably) low-spin $[Fe(TPP)(py)_2]^+$.

The synthesis of Fe(OEP)(py)(NCS) as a means of obtaining a derivative with higher spin multiplicity than Fe(TPP)(py)(NCS) was made because we have previously observed[26] that OEP complexes frequently have higher spin states than the TPP analogues. Further studies into the question of how the spin state of (porphinato)iron complexes are influenced by the identity of the porphinato ligand are in progress.

Structure of Fe(TPP)(py)(NCS). Figure 2 is a perspective view of the Fe(TPP)(py)(NCS) molecule as it exists in the crystalline state. The nonlinear Fe–NCS group is clearly seen. Figure 2 also displays the atom labels assigned and used in Tables II, III, VI, and VII. Individual values of bond distances and angles in the molecule are listed in Tables VI and VII, respectively. Figure 3 is a formal diagram of a porphinato core displaying the average values[27] for the chemically equivalent bond distances and angles in the porphinato core.

Figure 3 also displays the perpendicular displacements of the atoms of the porphinato core from the mean plane of the 24-atom core. The porphinato core has a pronounced S_4 ruffling which is, nonetheless, unremarkable in terms of porphinato core conformations observed.[28,29] The dihedral angles between the peripheral phenyl groups and the core are 60.3, 77.5, 61.7, and 72.2°. The iron(III) atom is slightly displaced (0.05 Å), out of plane, toward the isothiocyanato ligand.

The coordination group bond distances (Figure 2) are consistent with a low-spin iron(III) porphyrinate species. The average Fe–N_p distance of 1.988 (9) Å is essentially identical with the 1.990-Å average value observed in eight other low-spin iron(III) porphyrinates.[30] The axial Fe–N(py) distance (2.082 (3) Å) observed in Fe(TPP)(py)(NCS) is similar to the 2.089 (6) Å in low-spin $Fe(TPP)(N_3)(py)$,[23] the 2.075 (3) Å value for Fe(TPP)(CN)(py),[24] and the 2.031 (2) Å value in the low-spin form[26] of $[Fe(OEP)(3\text{-}Clpy)_2]ClO_4$. All of these distances are considerably smaller than the 2.316 (5) Å value for Fe-N(py) in the high-spin form[26] of $[Fe(OEP)(3\text{-}Clpy)_2]ClO_4$.

The axial Fe–N(NCS) distance is 1.942 (4) Å. This distance is slightly shorter than the 1.957 (5) Å distance observed[10] in high-spin Fe(TPP)(NCS) and significantly shorter than the average 2.002-Å distances observed[31] in high-spin $FeL_1(NCS)_2ClO_4$ and $FeL_2(NCS)_2ClO_4$, where L_1 and L_2 are 15- and 16-membered pentadentate macrocycles. Similarly, the Fe–N distance in hexakis(isothiocyanato)ferrate(III)[32] of 2.047 Å is substantially longer than that observed in Fe(TPP)(py)(NCS).

Table VII. Bond Angles (Deg) in the FeTPP(py)(NCS) Molecule[a]

N_1FeN_2	89.8 (1)	$N_4C_{a8}C_{b8}$	109.3 (3)
N_1FeN_3	177.2 (1)	$C_{m4}C_{a8}C_{b8}$	123.5 (3)
N_1FeN_4	90.4 (1)	$C_{a2}C_{m1}C_{a3}$	123.7 (3)
N_1FeN_5	87.8 (1)	$C_{a2}C_{m1}C_1$	117.5 (3)
N_1FeN_6	92.7 (1)	$C_{a3}C_{m1}C_1$	118.5 (3)
N_2FeN_3	90.5 (1)	$C_{a4}C_{m2}C_{a5}$	123.0 (3)
N_2FeN_4	177.8 (1)	$C_{a4}C_{m2}C_7$	117.5 (3)
N_2FeN_5	90.6 (1)	$C_{a5}C_{m2}C_7$	119.3 (3)
N_2FeN_6	93.0 (1)	$C_{a6}C_{m3}C_{a7}$	122.4 (3)
N_3FeN_4	89.2 (1)	$C_{a6}C_{m3}C_{13}$	118.2 (3)
N_3FeN_5	89.4 (1)	$C_{a7}C_{m3}C_{13}$	119.3 (3)
N_3FeN_6	90.1 (1)	$C_{a1}C_{m4}C_{a8}$	122.3 (3)
N_4FeN_5	87.2 (1)	$C_{a1}C_{m4}C_{19}$	119.4 (3)
N_4FeN_6	89.1 (1)	$C_{a8}C_{m4}C_{19}$	118.2 (3)
N_5FeN_6	176.3 (1)	$C_{a1}C_{b1}C_{b2}$	107.0 (3)
$C_{a1}N_1C_{a2}$	106.1 (3)	$C_{a2}C_{b2}C_{b1}$	107.9 (3)
$C_{a3}N_2C_{a4}$	106.8 (3)	$C_{a3}C_{b3}C_{b4}$	108.5 (3)
$C_{a5}N_3C_{a6}$	106.1 (3)	$C_{a4}C_{b4}C_{b3}$	107.0 (3)
$C_{a7}N_4C_{a8}$	106.6 (3)	$C_{a5}C_{b5}C_{b6}$	107.4 (3)
$N_1C_{a1}C_{m4}$	125.5 (3)	$C_{a6}C_{b6}C_{b5}$	107.4 (3)
$N_1C_{a1}C_{b1}$	109.8 (3)	$C_{a7}C_{b7}C_{b8}$	107.3 (3)
$C_{m4}C_{a1}C_{b1}$	124.6 (3)	$C_{a8}C_{b8}C_{b7}$	107.5 (3)
$N_1C_{a2}C_{m1}$	125.3 (3)	$C_{25}N_5C_{29}$	116.9 (3)
$N_1C_{a2}C_{b2}$	109.2 (3)	$N_5C_{25}C_{26}$	122.8 (4)
$C_{m1}C_{a2}C_{b2}$	125.3 (3)	$C_{25}C_{26}C_{27}$	118.6 (5)
$N_2C_{a3}C_{m1}$	125.7 (3)	$C_{26}C_{27}C_{28}$	119.2 (4)
$N_2C_{a3}C_{b3}$	108.4 (3)	$C_{27}C_{28}C_{29}$	119.6 (4)
$C_{m1}C_{a3}C_{b3}$	125.6 (3)	$C_{28}C_{29}N_5$	122.9 (4)
$N_2C_{a4}C_{m2}$	126.7 (3)	$N_6C_{30}S$	177.0 (4)
$N_2C_{a4}C_{b4}$	109.2 (3)	FeN_1C_{a1}	126.3 (2)
$C_{m2}C_{a4}C_{b4}$	124.0 (3)	FeN_1C_{a2}	127.0 (2)
$N_3C_{a5}C_{m2}$	125.7 (3)	FeN_2C_{a3}	126.6 (2)
$N_3C_{a5}C_{b5}$	109.2 (3)	FeN_2C_{a4}	126.2 (2)
$C_{m2}C_{a5}C_{b5}$	124.7 (3)	FeN_3C_{a5}	126.8 (2)
$N_3C_{a6}C_{m3}$	125.4 (3)	FeN_3C_{a6}	127.1 (2)
$N_3C_{a6}C_{b6}$	109.7 (3)	FeN_4C_{a7}	126.8 (2)
$C_{m3}C_{a6}C_{b6}$	124.8 (3)	FeN_4C_{a8}	126.2 (2)
$N_4C_{a7}C_{m3}$	125.6 (3)	FeN_5C_{25}	121.7 (3)
$N_4C_{a7}C_{b7}$	109.2 (3)	FeN_5C_{29}	121.2 (3)
$C_{m3}C_{a7}C_{b7}$	124.9 (3)	FeN_6C_{30}	155.6 (3)
$N_4C_{a8}C_{m4}$	127.0 (3)		

[a] The numbers in parentheses are the estimated standard deviations in the least significant figure.

The angle between the two axial nitrogen ligands is nearly linear with N_5–Fe–N_6 = 176.3 (1)°. The pyridine ring is oriented in a generally favorable fashion: the angle between the normals to the pyridine plane and the coordinate plane N_5FeN_1 is 39°, a value of 45° leads to minimum steric interaction between the pyridine and the porphinato core.

As noted previously, the Fe–NCS group is decidedly nonlinear; the observed Fe–N_6–C_{30} angle is 155.6 (3)°. The N_6–C_{30}–S group is effectively linear with an angle of 177.0 (4)°. The N_6–C_{30} and C_{30}–S separations, 1.144 (5) and 1.606 (5) Å, respectively, are normal. The bending of the Fe–NCS group can be ascribed to packing considerations. In the observed crystal structure, the closest intermolecular approaches of the thiocyanate atoms and atoms of adjacent molecules are $C_{30}\cdots C_{28}$ = 3.51 Å, $C_{30}\cdots C_{27}$ = 3.52 Å, and $S\cdots C_{10}$ = 3.77 Å. For the hypothetical molecule having the same crystal structure but a linear Fe–NCS group, these nonbonded distances decrease to 3.28, 3.14, and 2.86 Å. The hypothetical $S\cdots C_{10}$ contact is especially unreasonable. Since the intermolecular packing arrangement of a large molecule such as Fe(TPP)(py)(NCS) is unlikely to be dominated by the packing relationships of one axial ligand, the hypothesis that the bending

(26) Scheidt, W. R.; Haller, K. J.; Geiger, D. K. *J. Am. Chem. Soc.* **1982**, *104*, 495–499.
(27) The numbers in parentheses for these and other averaged values are the estimated standard deviations calculated on the assumption that the individual values are drawn from the same population.
(28) Board, J. L. In "Porphyrins and Metalloporphyrins"; Smith, K. M., Ed.; Elsevier: Amsterdam, 1975; pp 317–380.
(29) Scheidt, W. R. *Porphyrins* **1978**, *3*, 463–511.
(30) Scheidt, W. R.; Reed, C. A. *Chem. Rev.* **1981**, *81*, 543–555.
(31) Drew, M. G. B.; Othman, A. H.; McIlroy, P. D. A.; Nelson, S. M. *J. Chem. Soc., Dalton Trans.* **1975**, 2507–2516.
(32) Muller, V. U. *Acta Crystallogr., Sect. B* **1977**, *B33*, 2197–2201.

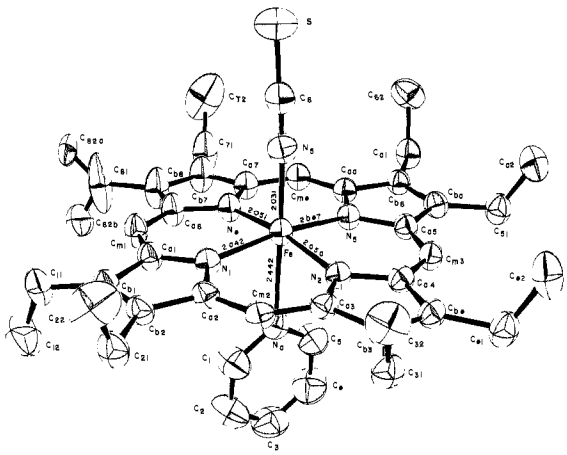

Figure 4. An ORTEP drawing of the Fe(OEP)(py)(NCS) molecule showing the atom labeling scheme and bond distances in the coordination group. The 50% probability ellipsoids are shown.

Table VIII. Bond Lengths (Å) in the Fe(OEP)(py)(NCS) Molecule[a]

Fe–N_1	2.042 (2)	C_{a2}–C_{b2}	1.448 (3)	C_{b5}–C_{b6}	1.367 (3)
Fe–N_2	2.050 (2)	C_{a2}–C_{m2}	1.390 (3)	C_{b5}–C_{51}	1.506 (3)
Fe–N_3	2.047 (2)	C_{a3}–C_{b3}	1.453 (3)	C_{b6}–C_{61}	1.497 (3)
Fe–N_4	2.051 (2)	C_{a3}–C_{m2}	1.398 (3)	C_{b7}–C_{b8}	1.357 (4)
Fe–N_5	2.031 (2)	C_{a4}–C_{b4}	1.448 (3)	C_{b7}–C_{71}	1.514 (4)
Fe–N_6	2.442 (2)	C_{a4}–C_{m3}	1.387 (3)	C_{b8}–C_{81}	1.523 (4)
N_1–C_{a1}	1.371 (3)	C_{a5}–C_{b5}	1.442 (3)	C_{11}–C_{12}	1.494 (5)
N_1–C_{a2}	1.373 (3)	C_{a5}–C_{m3}	1.398 (3)	C_{21}–C_{22}	1.501 (5)
N_2–C_{a3}	1.369 (3)	C_{a6}–C_{b6}	1.447 (3)	C_{31}–C_{32}	1.508 (4)
N_2–C_{a4}	1.376 (3)	C_{a6}–C_{m4}	1.388 (3)	C_{41}–C_{42}	1.512 (4)
N_3–C_{a5}	1.374 (3)	C_{a7}–C_{b7}	1.437 (3)	C_{51}–C_{52}	1.498 (4)
N_3–C_{a6}	1.382 (3)	C_{a7}–C_{m4}	1.386 (3)	C_{61}–C_{62}	1.508 (4)
N_4–C_{a7}	1.379 (3)	C_{a8}–C_{b8}	1.447 (3)	C_{71}–C_{72}	1.466 (6)
N_4–C_{a8}	1.374 (3)	C_{a8}–C_{m1}	1.391 (3)	C_{81}–C_{82a}	1.190 (7)
N_5–C_6	1.153 (3)	C_{b1}–C_{b2}	1.360 (3)	C_{81}–C_{82b}	1.208 (7)
N_6–C_1	1.332 (4)	C_{b1}–C_{11}	1.503 (3)	C_1–C_2	1.373 (4)
N_6–C_5	1.329 (4)	C_{b2}–C_{21}	1.512 (3)	C_2–C_3	1.381 (5)
C_6–S	1.626 (3)	C_{b3}–C_{b4}	1.359 (3)	C_3–C_4	1.346 (5)
C_{a1}–C_{b1}	1.437 (3)	C_{b3}–C_{31}	1.507 (3)	C_4–C_5	1.370 (4)
C_{a1}–C_{m1}	1.395 (3)	C_{b4}–C_{41}	1.500 (3)		

[a] The numbers in parentheses are the estimated standard deviations in the least significant figure.

of the Fe–NCS group is caused by intermolecular forces appears reasonable.

We have also examined the inter- and intramolecular packing contacts in a number[31-33] of isothiocyanato complexex having M–N–C angles in the range 140–160°. In all cases, substantially smaller nonbonded contacts involving the thiocyanate were observed for the *hypothetical* crystal structure containing a linear M–NCS group than in the *observed* crystal structure containing the bent group.[34] Thus packing considerations may play a role in these bent M–NCS groups as well.

(33) (a) $K_2Co(NCS)_4$: Drew, M. G. B.; Othman, A. H. *Acta Crystallogr., Sect. B* **1975**, *B31*, 613–614. (b) $(NH_4)_2VO(NCS)_4$: Hazell, A. C. *J. Chem. Soc.* **1963**, 5745–5751. (c) $Co(C_{19}H_{15}N_5O)(NCS)_2$: Mangia, A.; Nardelli, M.; Pelizzi, G. *Acta Crystallogr., Sect. B* **1974**, *B30*, 487–491. (d) $Zn_2(C_{10}H_{14}N_2O)_2(NCS)_4$: Bigoli, F.; Braibanti, A.; Pellinghelli, M. A.; Tiripicchio, A. *Ibid.* **1973**, *B29*, 2708–2712. (e) $Mn_2(C_3H_5N_3)_5(NCS)_4$: Englefreit, D. W.; Vershoor, G. C.; Vermin, W. J. *Ibid.* **1979**, *B35*, 2927–2931. (f) Ni(4-Mepy)$_4$(NCS)$_2$: Kerr, I. S.; Williams, D. J. **1977**, *B33*, 3589–3592. (g) Fe(py)$_4$(NCS)$_2$: Søtfote, I.; Rasmussen, S. E. *Acta Chem. Scand.* **1967**, *21*, 2028–2040. (h) Cd(bis(2-aminoethyl)amine)(NCS)$_2$: Cannas, M.; Carta, G.; Cristini, A.; Marongiu, G. *Inorg. Chem.* **1977**, *16*, 228–230. (i) Sn(terpy)$(CH_3)_2$(NCS)$_2$: Naik, D. V.; Scheidt, W. R. *Inorg. Chem.* **1973**, *12*, 272–276. (j) $FeL_1(NCS)_2$ and $FeL_2(NCS)_2$: Drew, M. G. B.; Othman, A. H.; Nelson, S. M. *J. Chem. Soc., Dalton Trans.* **1976**, 1394–1399.

(34) In all the hypothetical structures, i.e., with a linear M–NCS group rather than the observed nonlinear group, at least one unrealistically close nonbonded contact with the terminal S atom of the thiocyanate was found. The calculated S···X contacts ranged from 2.2 Å upward. Corresponding distances in the observed crystal structures were never calculated to be unreasonable.

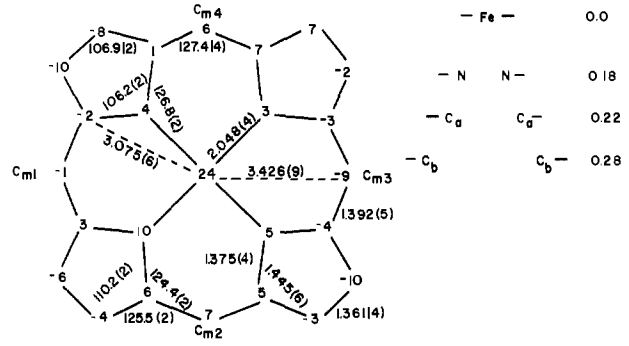

Figure 5. A formal diagram of the porphinato core of Fe(OEP)(py)(NCS) is displayed on the left-hand side. Each atom label of this figure, which has the same orientation as Figure 4, has been replaced by the value of the perpendicular displacement, in units of 0.01 Å, of the atom from the mean plane of the 24-atom core. The right-hand side of the diagram displays the displacement of the iron atom from the best planes of the four nitrogen atoms, the eight α-pyrrole carbon atoms, and the eight β-pyrrole carbon atoms.

Table IX. Bond Angles (Deg) in the Fe(OEP)(py)(NCS) Molecule[a]

N_1FeN_2	89.7 (1)	FeN_4C_{a7}	127.1 (2)
N_1FeN_3	170.5 (1)	FeN_4C_{a8}	126.6 (2)
N_1FeN_4	90.0 (1)	$C_{a7}N_4C_{a8}$	106.2 (2)
N_1FeN_5	94.4 (1)	FeN_5C_6	176.0 (2)
N_1FeN_6	83.0 (1)	FeN_6C_1	122.6 (2)
N_2FeN_3	89.4 (1)	FeN_6C_5	121.2 (2)
N_2FeN_4	169.0 (1)	$C_{a1}C_{m1}C_{a8}$	128.0 (2)
N_2FeN_5	96.5 (1)	$C_{a2}C_{m2}C_{a3}$	126.9 (2)
N_2FeN_6	84.3 (1)	$C_{a4}C_{m3}C_{a5}$	127.3 (2)
N_3FeN_4	89.1 (1)	$C_{a6}C_{m4}C_{a7}$	127.3 (2)
N_3FeN_5	95.1 (1)	$N_1C_{a1}C_{m1}$	124.3 (2)
N_3FeN_6	87.4 (1)	$N_1C_{a1}C_{b1}$	110.2 (2)
N_4FeN_5	94.5 (1)	$C_{m1}C_{a1}C_{b1}$	125.5 (2)
N_4FeN_6	84.7 (1)	$N_1C_{a2}C_{m2}$	124.8 (2)
N_5FeN_6	177.3 (1)	$N_1C_{a2}C_{b2}$	109.5 (2)
N_5C_6S	179.6 (2)	$C_{m2}C_{a2}C_{b2}$	125.6 (2)
FeN_1C_{a1}	126.8 (1)	$N_2C_{a3}C_{m2}$	124.6 (2)
FeN_1C_{a2}	126.8 (1)	$N_2C_{a3}C_{b3}$	110.2 (2)
$C_{a1}N_1C_{a2}$	106.5 (2)	$C_{m2}C_{a3}C_{b3}$	125.2 (2)
FeN_2C_{a3}	126.7 (1)	$N_2C_{a4}C_{m3}$	124.5 (2)
FeN_2C_{a4}	127.0 (1)	$N_2C_{a4}C_{b4}$	110.0 (2)
$C_{a3}N_2C_{a5}$	106.2 (2)	$C_{m2}C_{a3}C_{b3}$	125.4 (2)
FeN_3C_{a5}	127.1 (1)	$N_3C_{a5}C_{m3}$	124.3 (2)
FeN_3C_{a6}	126.4 (1)	$N_3C_{a5}C_{b5}$	110.2 (2)
$C_{a5}N_3C_{a6}$	106.1 (2)	$C_{m3}C_{a5}C_{b5}$	125.5 (2)
$N_3C_{a6}C_{m4}$	124.6 (2)	$C_{a8}C_{b8}C_{b7}$	106.7 (2)
$N_3C_{a6}C_{b6}$	109.9 (2)	$C_{11}C_{b1}C_{b2}$	127.7 (2)
$C_{m4}C_{a6}C_{b6}$	125.4 (2)	$C_{21}C_{b2}C_{b1}$	127.6 (2)
$N_4C_{a7}C_{m4}$	124.2 (2)	$C_{31}C_{b3}C_{b4}$	128.8 (2)
$N_4C_{a7}C_{b7}$	109.9 (2)	$C_{41}C_{b4}C_{b3}$	128.1 (2)
$C_{m4}C_{a7}C_{b7}$	125.9 (2)	$C_{51}C_{b5}C_{b6}$	127.8 (2)
$N_4C_{a8}C_{m1}$	124.2 (2)	$C_{61}C_{b6}C_{b5}$	128.7 (2)
$N_4C_{a8}C_{b8}$	109.9 (2)	$C_{71}C_{b7}C_{b8}$	127.8 (2)
$C_{m1}C_{a8}C_{b8}$	125.9 (2)	$C_{81}C_{b8}C_{b7}$	128.8 (2)
$C_{a1}C_{b1}C_{11}$	125.5 (2)	$C_{b1}C_{11}C_{12}$	113.4 (3)
$C_{a1}C_{b1}C_{b2}$	106.8 (2)	$C_{b2}C_{21}C_{22}$	113.0 (2)
$C_{a2}C_{b2}C_{21}$	125.4 (2)	$C_{b3}C_{31}C_{32}$	112.6 (2)
$C_{a2}C_{b2}C_{b1}$	107.0 (2)	$C_{b4}C_{41}C_{42}$	114.0 (2)
$C_{a3}C_{b3}C_{31}$	124.6 (2)	$C_{b5}C_{51}C_{52}$	113.0 (2)
$C_{a3}C_{b3}C_{b4}$	106.6 (2)	$C_{b6}C_{61}C_{62}$	112.2 (2)
$C_{a4}C_{b4}C_{41}$	125.0 (2)	$C_{b7}C_{71}C_{72}$	114.3 (3)
$C_{a4}C_{b4}C_{b3}$	106.9 (2)	$C_{b8}C_{81}C_{82a}$	126.0 (6)
$C_{a5}C_{b5}C_{51}$	125.2 (2)	$C_{b8}C_{81}C_{82b}$	120.1 (5)
$C_{a5}C_{b5}C_{b6}$	107.0 (2)	$N_6C_1C_2$	123.5 (3)
$C_{a6}C_{b6}C_{61}$	124.6 (2)	$C_1C_2C_3$	118.9 (3)
$C_{a6}C_{b6}C_{b5}$	106.6 (2)	$C_2C_3C_4$	117.9 (3)
$C_{a7}C_{b7}C_{71}$	124.9 (2)	$C_3C_4C_5$	120.0 (3)
$C_{a7}C_{b7}C_{b8}$	107.3 (2)	$C_4C_5N_6$	123.5 (3)
$C_{a8}C_{b8}C_{81}$	124.4 (2)	$C_1N_6C_5$	116.2 (2)

[a] The numbers in parentheses are the estimated standard deviations in the least significant figure.

However, for packing constraints to have a substantial part in the observed geometry of the moiety, the force constant for bending

the normally linear M–N–C group must be relatively low. Drew et al.[33j] suggest that nonlinear arrangements for M–NCS will be favored where the metal is a poor π donor to the isothiocyanate ligand. We have previously noted[35] that in $[Fe(TPP)(CN)_2]^-$ the relatively long Fe–C distances suggests that even the strong π-acceptor ligand cyanide can not compete with the porphinato ligand for metal π density. Thus the condition suggested by Drew et al. for a nonlinear M–NCS group is met in the iron(III) porphyrinate complexes. We believe however, in accord with the observation of Bloom and Hoard[10] and our observations of Fe(OEP)(py)(NCS) (vide infra), that a linear M–NCS geometry is the normal binding mode of isothiocyanate to iron(III) porphyrinates.

Structure of Fe(OEP)(py)(NCS). Figure 4 is a computer-drawn model of the Fe(OEP)(py)(NCS) molecule. This figure displays the atom labels used in Tables IV, V, VIII, and IX. Individual values of bond distances and angles in this molecule are listed in Tables VIII and IX, respectively. Figure 5 is a formal diagram of the porphinato core in Fe(OEP)(py)(NCS) displaying the average values of chemically equivalent bond distances and angles. Important radii involving iron are also displayed.

The left-hand side of Figure 5 also displays the perpendicular displacements of the atoms of the core from the mean plane of the 24-atom core. The high-spin iron(III) atom is displaced by 0.24 Å from this plane toward the coordinated isothiocyanate ligand. The porphinato core has a conformation that approaches that of a C_{4v} domed core. The right-hand side of Figure 5 gives the displacement of the iron(III) atom from the best planes of the four pyrrole nitrogen atoms, the eight α-pyrrole carbon atoms, and the eight β-pyrrole carbon atoms.

The coordination group bond distances of Fe(OEP)(py)(NCS) are displayed in Figure 4 and are clearly different than those of Fe(TPP)(py)(NCS). The average Fe–N_p distance of 2.048 (4) Å are quite close to those observed[26,35,36] for other high-spin six-coordinate ferric porphyrinates. The average value observed in these complexes is 2.045 Å. There is one significant difference between these complexes and Fe(OEP)(py)(NCS). All previously characterized six-coordinate high-spin species had two identical axial ligands; the present complex does not. As a consequence of the equivalent axial ligands, the iron(III) atom was centered in the central hole of the porphinate core. The large high-spin iron(III) atom was accommodated by a radial expansion of the core. However, in Fe(OEP)(py)(NCS), the large iron(III) atom is accommodated by a combination of core expansion and displacement of the iron(III) atom from the mean plane of the core. The radial expansion of the core is given by the center of the hole to nitrogen distance of 2.034 Å. This is a significant increase over the ~1.990-Å value seen in the low-spin ferric complexes.

Presumably, the displacement of the iron atom is dependent, at least in part, on the relative importance of the bonding of the two dissimilar axial ligands. Some measure of the asymmetry in axial ligand binding can be seen in the difference in axial bond lengths. The Fe–N(NCS) distance of 2.031 (2) Å is similar to that of other high-spin ferric complexes noted previously.[31,32] The axial Fe–N(py) distance of 2.442 (2) Å is significantly longer than the Fe–N(py) distances of the low-spin porphinato derivatives described earlier and indeed can be described as "semicoordinated". This distance is also significantly longer than the 2.316 (5) Å distance observed[26] in the high-spin form of $[Fe(OEP)(3\text{-}Clpy)_2]ClO_4$. The axial bond distances are thus consistent with a substantially stronger bond to the isothiocyanato ligand and, as noted, the iron(III) atom is displaced 0.24 Å from the mean plane toward this ligand.

The difference in the average bond length of low-spin Fe(TPP)(py)(NCS) (1.996) and high-spin Fe(OEP)(py)(NCS) (2.111) is 0.115 Å. This value is quite close to the 0.13-Å difference in the low- and high-spin forms[26] of $[Fe(OEP)(3\text{-}Clpy)_2]ClO_4$ and other six-coordinate d^5 Fe(III) complexes that exist in $S = {}^1/_2$ and $S = {}^5/_2$ forms. Bond length changes of this magnitude are found in tridentate N_4O_2 complexes,[38] hexadentate N_4O_2 complexes,[39] and dithiocarbamate complexes.[40,41]

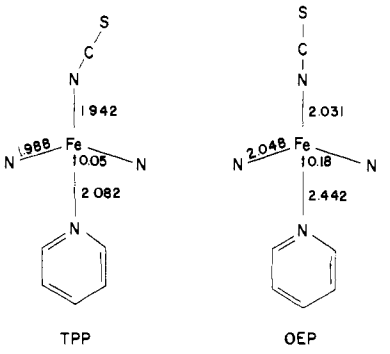

Figure 6. A schematic diagram illustrating the structural differences between the low-spin Fe(TPP)(py)(NCS) and high-spin Fe(OEP)(py)(NCS) molecules.

The angle between the two axial nitrogen ligands is nearly linear with N_5–Fe–N_6 = 177.3 (1)°. The pyridine ring orientation is almost 45° different than it is in Fe(TPP)(py)(NCS); the angle between the pyridine plane and the coordinate plane N_6FeN_1 is 4.2°. This orientation would lead to severe nonbonded contacts between the α-hydrogen atoms of the pyridine and porphinato nitrogen atoms if the Fe–N(py) distance was that appropriate for a low-spin complex. It is interesting to pose the question of whether this pyridine ring orientation is the result of, the cause of, or unrelated to the observed spin state. In Fe(OEP)(py)(NCS), the Fe–NCS group is essentially linear; the Fe–N_5–C_6 angle is 176.0 (2)°. The thiocyanate group is linear; the N_5–C_6–S angle is 179.6 (2)°. The N_5–C_6 distance is 1.153 (1) Å and C_6–S = 1.626 (3) Å. There are no unusual intermolecular contacts in Fe(OEP)(py)(NCS). Indeed it should be noted that the intermolecular separations in Fe(OEP)(py)(NCS) involving the linearly coordinated isothiocyanate ligand atoms are quite similar to those in the observed angularly coordinated thiocyanate of Fe(TPP)(py)(NCS).

Finally, some mention should be made concerning the Fe–N(NCS) bond lengths in low-spin Fe(TPP)(py)(NCS), high-spin Fe(OEP)(py)(NCS), and high-spin five-coordinate Fe(TPP)(NCS).[10] This bond distance in the latter complex is 1.957 Å, considerably closer to the low-spin value (1.942 Å) than the high-spin value. These results thus provide a direct confirmation of a suggestion made by Hoard[42] many years ago, namely, that the axial bond distance in high-spin five-coordinate iron(III) porphyrinates will be as short as expected for a low-spin complex.

Summary. The differences in structure of the low-spin and high-spin forms of Fe(Porph)(py)(NCS) are schematically illustrated in Figure 6. The average increase in Fe–ligand bond distances of 0.115 Å in the high-spin complex is expected. Less readily anticipated is the substantial anisotropy in the bond length differences with one bond, the Fe–N(py) bond, accounting for over half of the observed total increase. The magnitude of the displacement of the high-spin iron(III) atom from the mean plane of the core of Fe(OEP)(py)(NCS) is close to half that observed in five-coordinate high-spin iron(III) porphyrinates. The differences in structure of the two spin state forms of the Fe(Porph)(py)(NCS) molecules are probably the best structural

(35) Scheidt, W. R.; Haller, K. J.; Hatano, K. *J. Am. Chem. Soc.* **1980**, *102*, 6729–6735.
(36) Mashiko, T.; Kastner, M. E.; Spartalian, K.; Scheidt, W. R.; Reed, C. A. *J. Am. Chem. Soc.* **1978**, *100*, 6354–6362.
(37) Scheidt, W. R.; Cohen, I. A.; Kastner, M. E. *Biochemistry* **1979**, *18*, 3546–3552.
(38) Sim, P. G.; Sinn, E.; Petty, R. H.; Merrill, C. L.; Wilson, L. J. *Inorg. Chem.* **1981**, *20*, 1213–1222 and references therein.
(39) Sinn, E.; Sim, P. G.; Dose, E. V.; Tweedle, M. F.; Wilson, L. J. *J. Am. Chem. Soc.* **1978**, *100*, 3375–3390.
(40) Cukauskas, E. J.; Deaver, B. S., Jr.; Sinn, E. *J. Chem. Phys.* **1977**, *67*, 1257–1266 and references therein. Ewald, A. H.; Martin, R. L.; Sinn, E.; White, A. H. *Inorg. Chem.* **1969**, *9*, 1837–1846.
(41) Leipoldt, J. G.; Coppens, P. *Inorg. Chem.* **1973**, *12*, 2269–2274.
(42) Hoard, J. L. In "Structural Chemistry and Molecular Biology"; Rich, A.; Davidson, N.; Eds.; W. H. Freeman: San Francisco, CA; 1968; pp 573–594.

models to date of the expected changes in heme geometry for hemoproteins undergoing thermal spin equilibria. The question of whether the increased size of the high-spin iron(III) atom in the mixed-ligand derivatives will be accommodated by similar magnitudes of iron atom displacement and porphinato core expansion as observed in Fe(OEP)(py)(NCS) is a question being actively pursued.

Acknowledgment. We thank the National Institutes of Health for support of this work (at Notre Dame) under Grant HL-15627. We are grateful to Professors P. G. Rasmussen and Larry Garber for access to magnetic susceptibility apparatus. We thank Setsuko Kato for assistance with the NMR measurements.

Registry No. Fe(TPP)(py)(NCS)·$^1/_2$py, 81602-85-9; Fe(OEP)(py)(NCS), 81602-86-0.

Supplementary Material Available: Table III, anisotropic thermal parameters for Fe(TPP)(py)(NCS), Table V, anisotropic thermal parameters for Fe(OEP)(py)(NCS), and listings of observed and calculated structure amplitudes (×10) for Fe(TPP)(py)(NCS) and Fe(OEP)(py)(NCS) (51 pages). Ordering information is given on any current masthead page.

Adduct-Mediated Photochemistry. Evidence for Excited-State Reordering in (Acetophenone)tricarbonylchromium(0) upon Adduct Formation with Tris(6,6,7,7,8,8,8-heptafluoro-2,2-dimethyl-3,5-octanedionato)europium(III)

Rodney Schreiner and Arthur B. Ellis*

Contribution from the Department of Chemistry, University of Wisconsin-Madison, Madison, Wisconsin 53706. *Received November 5, 1981*

Abstract: The electronic spectra of several (arene)tricarbonylchromium(0) complexes (arene = aniline, anisole, benzaldehyde, benzene, acetophenone, acenaphthene) and the photochemical reactivity of the latter three species have been investigated in isooctane solution in the absence and presence of the title europium(III) β-diketonate complex, Eu(fod)$_3$. These complexes possess a band whose positional dependence on arene substituent leads to its assignment as predominantly Cr → arene charge transfer (MLCT). Addition of Eu(fod)$_3$ produced spectroscopic changes only for the acetophenone and benzaldehyde complexes, red-shifting the λ_{max} values of their MLCT bands by over 1000 cm^{-1} and shifting their IR terminal carbonyl stretching bands to higher energy by ~10 cm^{-1}. These spectral changes are ascribed to adduct formation wherein the arene carbonyl oxygen atom, serving as a site of Lewis basicity, coordinates to the Lewis acid, Eu(fod)$_3$. Spectrophotometric titrations support the presence of predominantly 1:1 adducts whose formation constants are ~10^3 M^{-1}. Visible and near-UV photolysis of the benzene, acetophenone, and acenaphthene complexes in 1-pentene/isooctane solution results in the disappearance of the complexes, presumably through photosubstitution of CO by 1-pentene, with quantum efficiencies, ϕ_d, of ~0.7, 0.2, and 0.001, respectively. Addition of Eu(fod)$_3$ affected ϕ_d for only the acetophenone complex: spectroscopic evidence indicates that the adduct undergoes the same photoreaction as the free complex but far less efficiently—ϕ_d is ~0.02. The decline in ϕ_d for the complexes examined roughly parallels the red-shift in their MLCT bands and is consistent with a model developed for other low-spin d^6 systems: the MLCT excited state is believed to be inert toward substitution; as it is tuned to below a ligand field excited state whose population leads to substitution, ϕ_d diminishes. The adduct photoreactivity is readily subsumed in this excited-state reordering model. Implications of adduct-mediated perturbation of excited-state properties are discussed.

Photochemists have recognized for some time that environment can profoundly affect molecular excited-state processes. Among the more well-studied sources of environmental perturbation are solvent, temperature, and heavy-atom effects.[1] Another technique for altering the molecular milieu is adduct formation. Although the excited-state properties of a number of complexes derived from organic constituents have been examined,[2] there are few such studies where one or both of the precursors is an organometallic species. A notable exception involves studies of the effect of adduct formation on the emissive properties of lanthanide β-diketonate complexes.[3] That adducts can be formed from a wide range of organometallic species has, of course, been amply demonstrated.[4]

Scheme I

$$A \xrightarrow{h\nu} B \quad (1)$$

$$A + M \rightleftharpoons AM \quad (2)$$

$$AM \xrightarrow{h\nu} \text{no reaction} \quad (3)$$

$$AM \xrightarrow{h\nu} CM \rightleftharpoons C + M \xrightarrow{-M} C \quad (4)$$

$$AM \xrightarrow{h\nu} BM \rightleftharpoons B + M \xrightarrow{-M} B \quad (5)$$

In searching for systems where the effects of adduct formation on photoreactions might be explored, we had the reactions of Scheme I in mind as possibilities. Ideally, we sought a photoreactive species, A, which would complex with a photoinert species, M, in a Lewis acid–base equilibrium, eq 2. If the adduct were

(1) Turro, N. J. "Modern Molecular Photochemistry"; Benjamin/Cummings: Menlo Park, Calif., 1978; e.g., Chapters 5, 6, and 8.
(2) Davidson, R. S. In "Molecular Association"; Foster, R.; Ed.; Academic Press: New York, 1975; Vol. I, Chapter 4, and references therein.
(3) See, for example: (a) Brittain, H. G. *Inorg. Chem.* **1980**, *19*, 640. (b) *J. Chem. Soc., Dalton Trans.* **1979**, 1187. (c) Brittain, H. G.; Richardson, F. S. *J. Am. Chem. Soc.* **1976**, *98*, 5858. (d) *J. Chem. Soc., Dalton Trans.* **1976**, 2253.
(4) See, for example: (a) Shriver, D. F. *Acc. Chem. Res.* **1970**, *3*, 231. (b) Marks, T. J.; Porter, R.; Kristoff, J. S.; Shriver, D. F. In "Nuclear Magnetic Resonance Shift Reagents"; Sievers, R. E.; Ed.; Academic Press: New York, 1973; p 247. (c) Drago, R. S. *Coord. Chem. Rev.* **1980**, *33*, 251. (d) Butts, S. B.; Strauss, S. H.; Holt, E. M.; Stimson, R. E.; Alcock, N. W.; Shriver, D. F. *J. Am. Chem. Soc.* **1980**, *102*, 5093.

0002-7863/82/1504-3374$01.25/0